iScience, Volume *23*

Supplemental Information

The Effect of CDK6 Expression on DNA Methylation and DNMT3B Regulation

Gerwin Heller, Sofie Nebenfuehr, Florian Bellutti, Huriye Ünal, Markus Zojer, Lisa Scheiblecker, Veronika Sexl, and Karoline Kollmann

SUPPLEMENTAL FIGURES

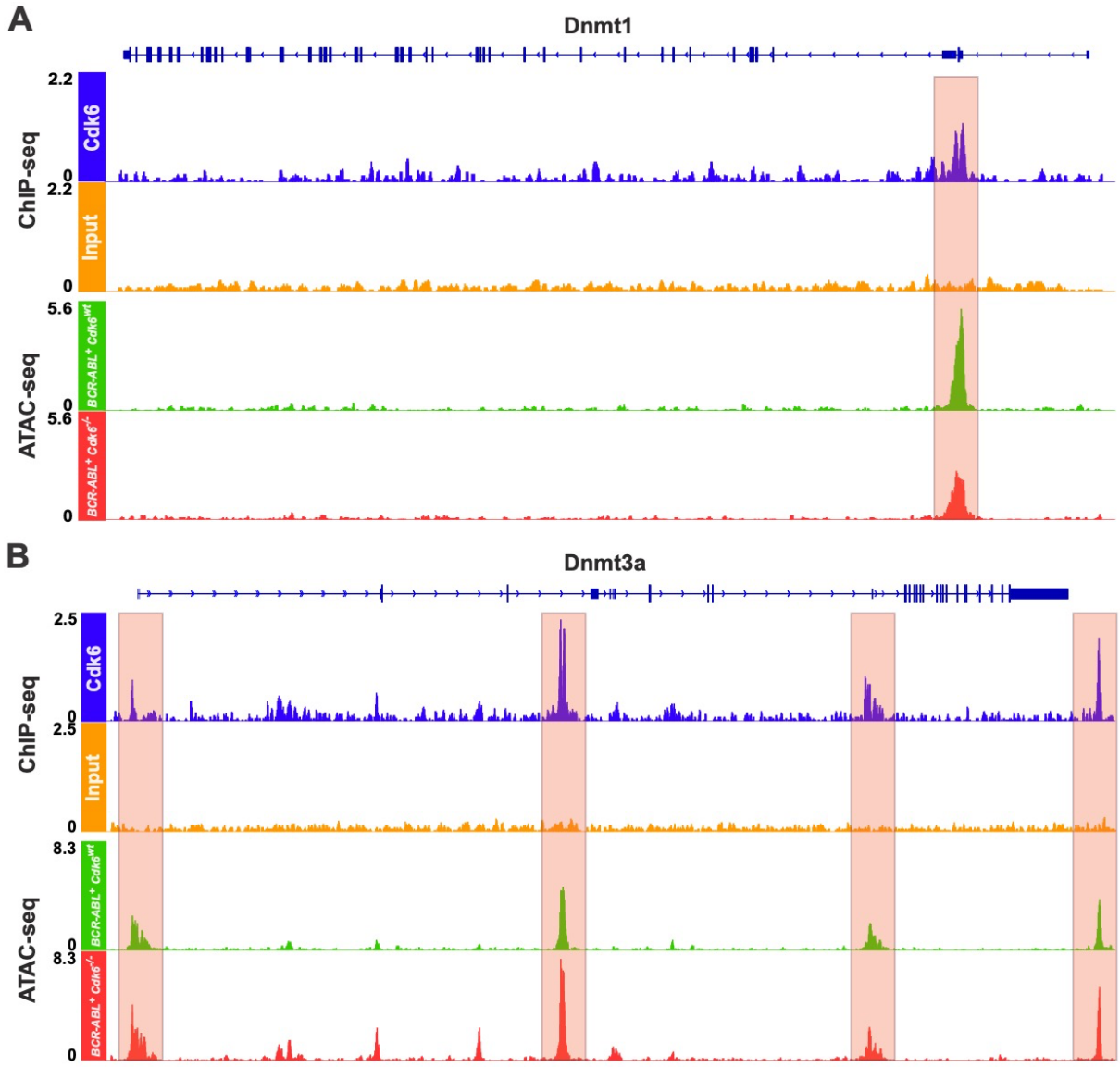

Figure S1, related to Figure 2. Binding of Cdk6 to the 5´ regions of **(A)** Dnmt1 and **(B)** Dnmt3a in *BCR-ABL*$^{+}$ cells determined by ChIP-seq analyses (upper panel). Chromatin accessibility at the 5´ regions of *Dnmt1 and Dnmt3a* in *BCR-ABL*$^{+}$ *Cdk6*^{wt} (green) and *BCR-ABL*$^{+}$ *Cdk6*$^{-/-}$ (red) cells determined by ATAC-seq analyses (lower panel).

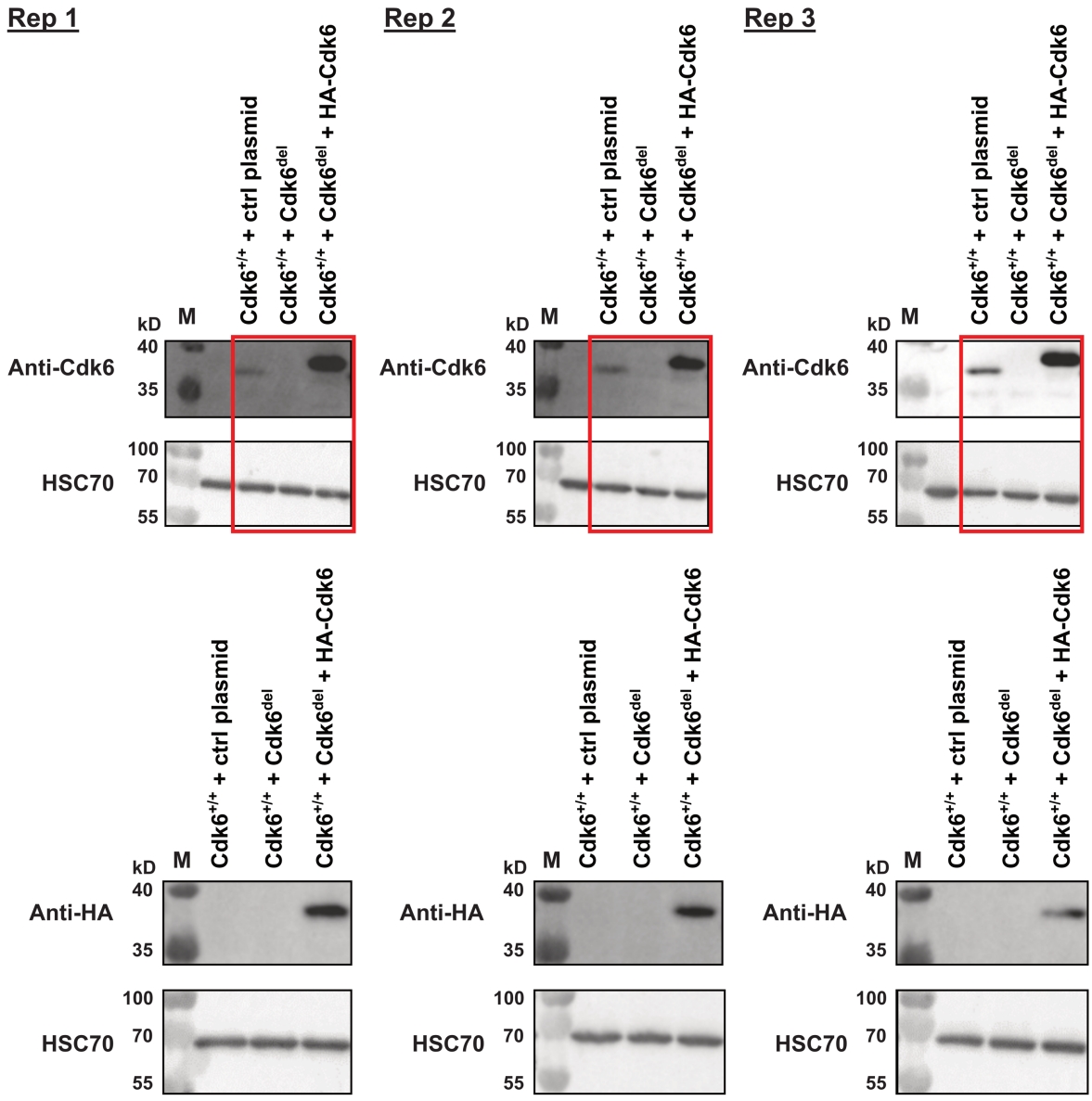

Figure S2, related to Figure 3. Western blot analyses to confirm Cdk6 loss and Cdk6 re-expression upon Cdk6 knock-out and HA-Cdk6 transduction, respectively. Results from 3 different cell lines (Rep 1-3) are shown. kD, kilodalton; M, marker.

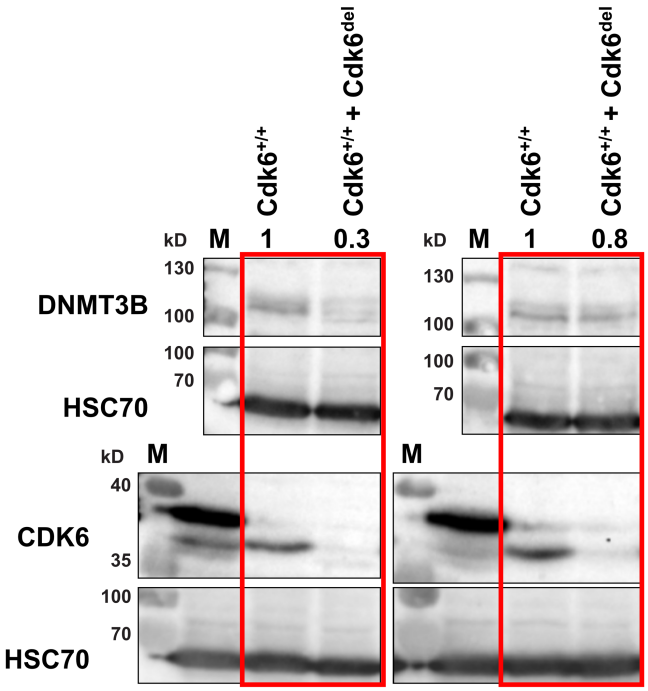

Figure S3, related to Figure 3. Western blot analyses of Dnmt3b and Cdk6 in *BCR-ABL*$^{+}$ *Cdk6*$^{+/+}$ and *BCR-ABL*$^{+}$ *Cdk6*$^{-/-}$ cell lines. Signals were densitometrically quantified and normalized to HSC70. kD, kilodalton; M, marker.

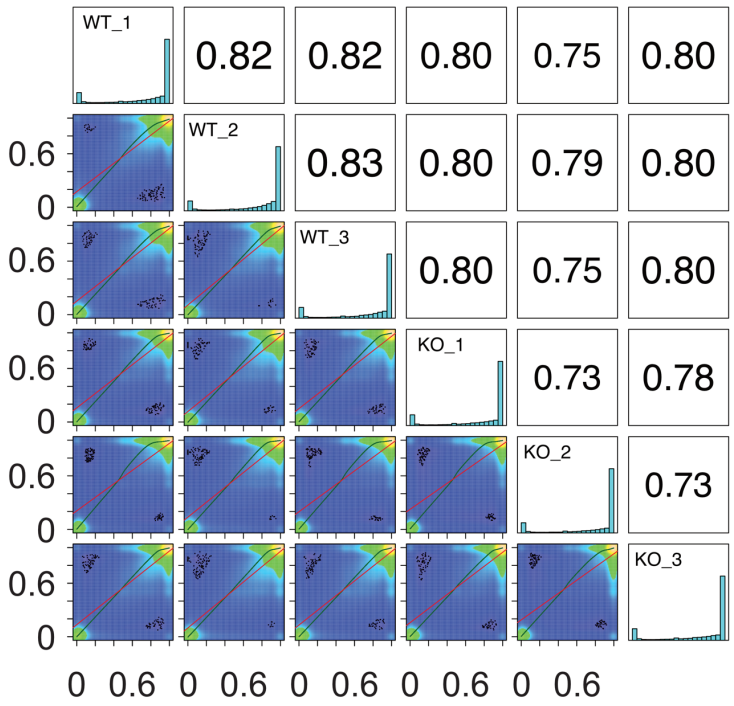

Figure S4, related to Figure 3. Correlation plot of 3 *BCR-ABL*$^{+}$ *Cdk6*^{wt} (WT) and 3 *BCR-ABL*$^{+}$ *Cdk6*$^{-/-}$ (KO) cell lines based on CpG methylation.

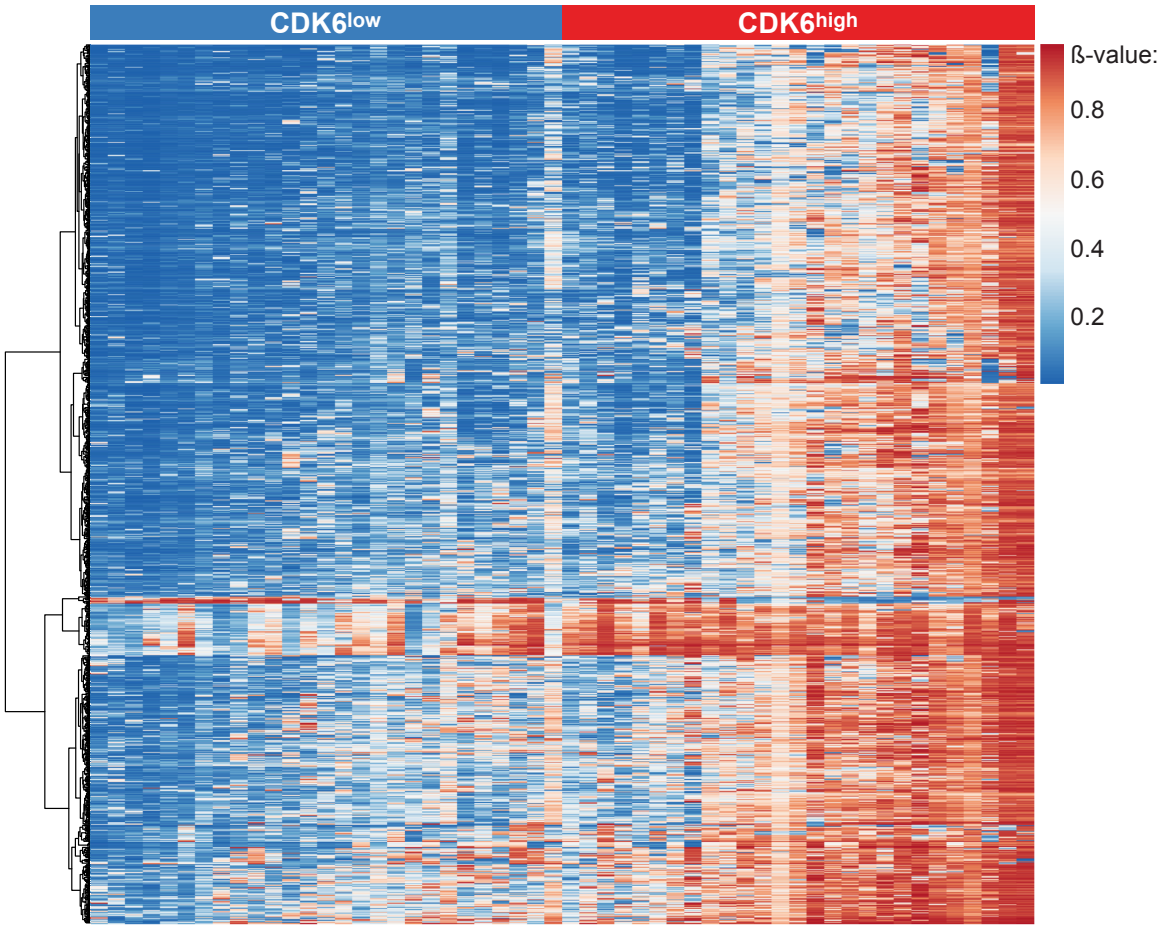

Figure S5, related to Figure 3. Heatmap showing methylation of 1,298 probes with a ß-difference of at least +/-0.3 between CDK6^{high} (upper quartile, N = 27) and CDK6^{low} (lower quartile, N = 27) AML samples from the TCGA LAML dataset. Values range from 0 (unmethylated; blue) to 1 (fully methylated; red). Each row represents a unique probe on the Infinium Human Methylation 450K BeadChip and each column represents a unique patient.

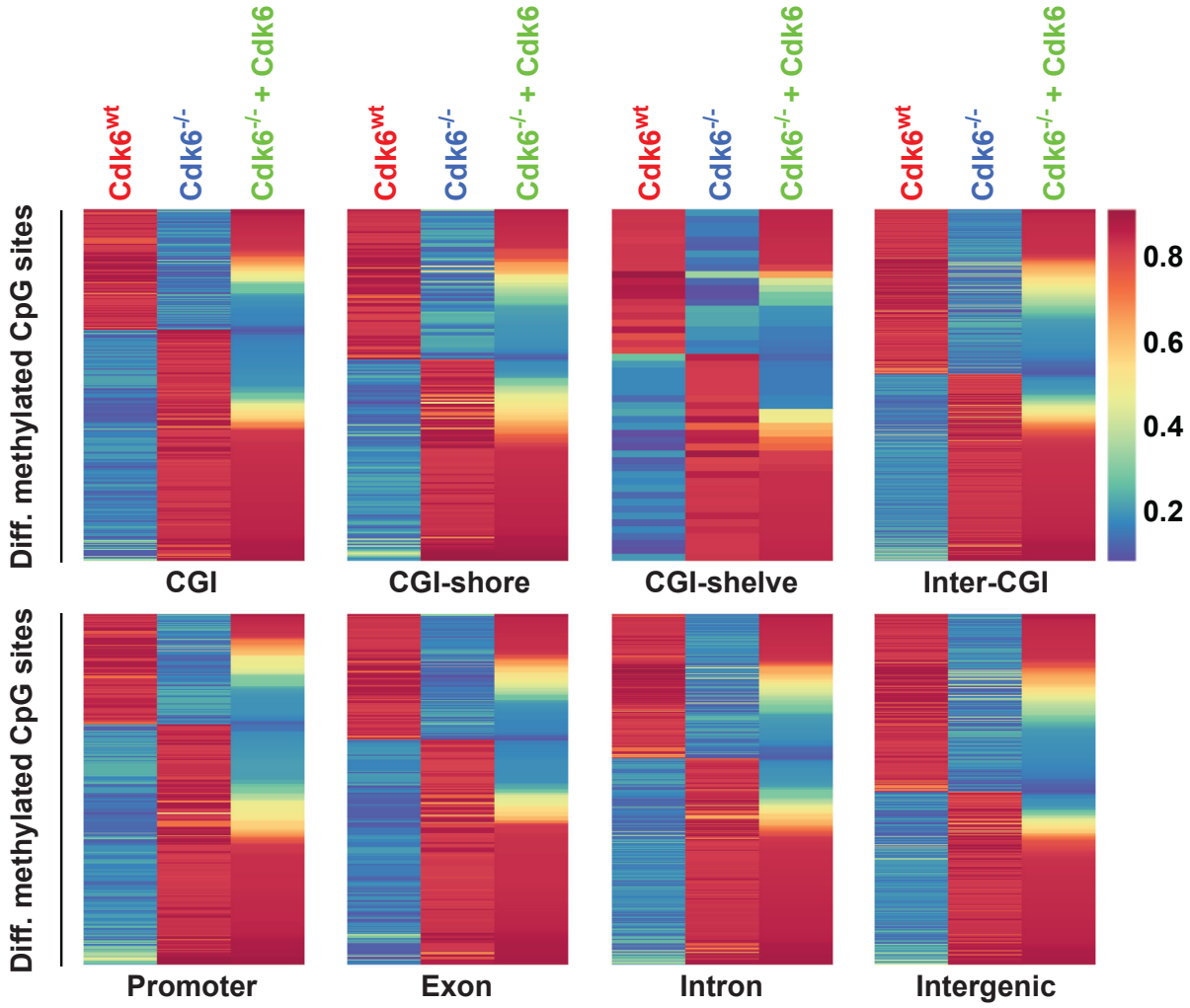

Figure S6, related to Figure 4. Heatmaps showing methylation values of differentially methylated CpG sites in 3 replicates (Rep 1-3) of *BCR-ABL*$^{+}$ *Cdk6*^{wt}, *BCR-ABL*$^{+}$ *Cdk6*$^{-/-}$ and *BCR-ABL*$^{+}$ *Cdk6*$^{-/-}$*+Cdk6* cell lines separated for CpG islands (CGI), CGI shores, CGI shelves, inter CGI regions, promoter regions, exons, introns and intergenic regions. Values are depicted as percentage of methylation and range from 0% (dark blue) to 100% (dark red).

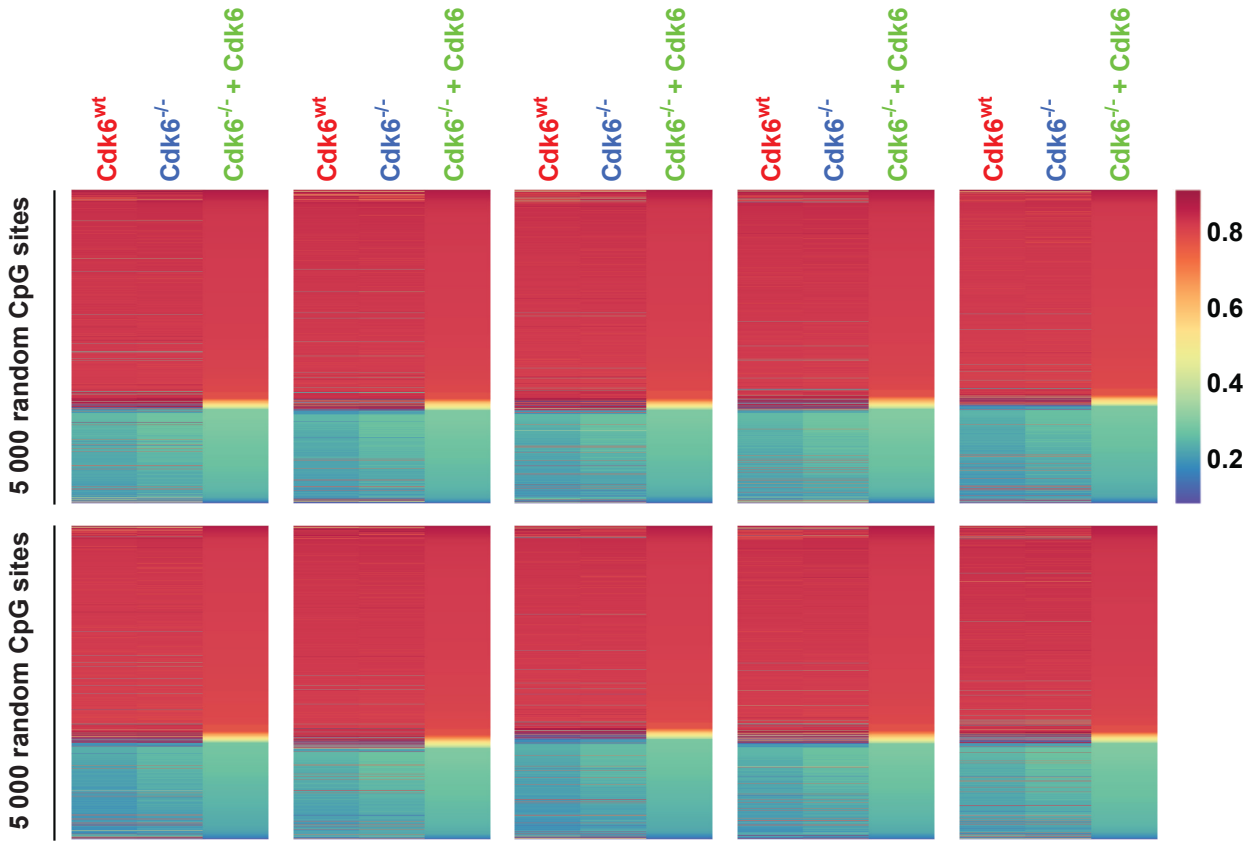

Figure S7, related to Figure 4. Heatmaps showing methylation values of 5 000 randomly selected CpG sites in *BCR-ABL*$^{+}$ *Cdk6*^{wt}, *BCR-ABL*$^{+}$ *Cdk6*$^{-/-}$ and *BCR-ABL*$^{+}$ *Cdk6*$^{-/-}$+*Cdk6* cell lines. Random CpG site selection was repeated for 10 times. Values are depicted as percentage of methylation and range from 0% (dark blue) to 100% (dark red).

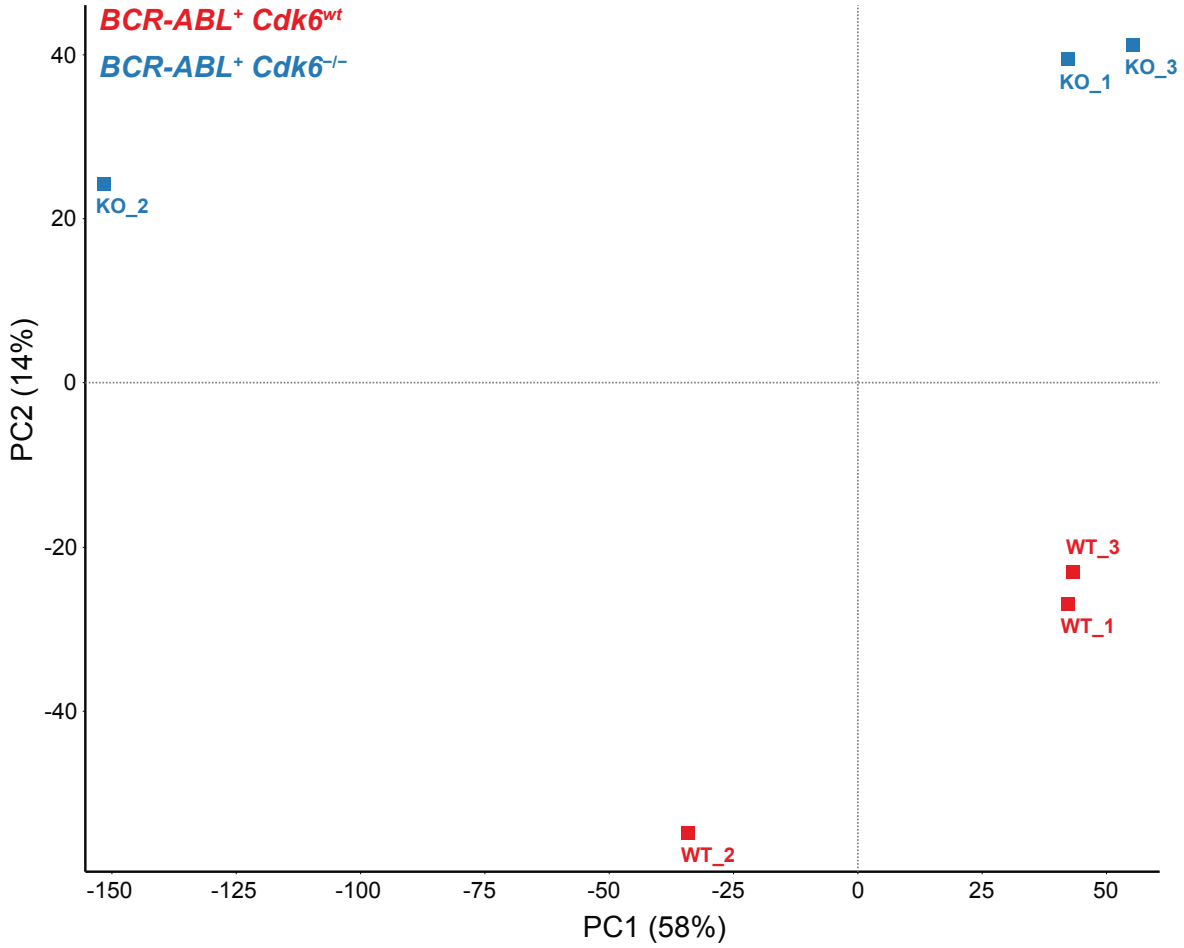

Figure S8, related to Figure 5. Principal component (PC) analysis of 3 *BCR-ABL*$^{+}$ *Cdk6*^{wt} (WT, red) and 3 *BCR-ABL*$^{+}$ *Cdk6*$^{-/-}$ (KO, blue) cell lines based on mRNA expression determined by RNA-sequencing.

TRANSPARENT METHODS

Cloning of CDK6 sgRNAs into px458 plasmid

pSpCas9(BB)-2A-GFP (px458) (plasmid number 48138; Addgene) was a gift from Krzysztof Chylinski. Cloning into px458 was performed as reported previously with slight modifications (Ran et al., 2013). The px458 plasmid was digested with BbsI (Thermofisher Scientific, Rockford, IL, USA) for 30 min at 37°C and gel purified using a Gel Extraction Kit (Qiagen, Hilden, Germany). The forward and reverse oligonucleotides (oligos) of each sgRNA were diluted at 100 µM in H_2O. The CDK6 guide oligos contain overhangs for ligation into the BbsI sites in pSpCas9(BB): forward CDK6 oligo: CACCGCCCGCGACTTGAAGAACGG, reverse CDK6 oligo: AAACCCGTTCTTCAAGTCGCGGGC. To phosphorylate and anneal the oligos, 2 µg of each oligo were mixed with T4 ligation buffer and T4 PNK (New England Biolabs, NEB, Ipswich, MA, USA) to a final volume of 20 µl and incubated for 1h at 37°C (phosphorylation), followed by 5 min at 95°C and then ramping down the temperature to 20°C at -1°C/min (annealing). Annealed and phosphorylated oligos were diluted 1:10 in H_2O. Ligation reactions for each sgRNA were performed by mixing 10 ng of the digested and purified px458 plasmid with 90 ng of the diluted phosphorylated and annealed oligos, T4 ligation buffer, and T4 ligase (NEB) in a final volume of 10 µl. Ligation was carried out for 16 h at 16°C. Chemically competent DHL5 bacteria were transformed and plated on LB plates containing 50 mg/ml ampicillin. Plates were incubated overnight at 37°C. Colonies were checked for correct insertion of the sgRNA by PCR colony screening, followed by sequencing (U6 primer: GAGGGCCTATTTCCCATGATTCC).

Gene editing in BCR-ABL+ cell lines

BCR-ABL+ cell lines were maintained in RPMI medium supplemented with 10% FCS, 50 µmol/L 2-mercaptoethanol, 100 U/mL penicillin, and 100 µg/mL streptomycin (PAA, Linz, Austria). Cells were electroporated (one single pulse with a voltage of 1600 V and a pulse width of 20 ms; NeonTM Transfection System, Invitrogen, Carlsbad, CA, USA) with 1µg control plasmid pSpCas9(BB)-2A-GFP(px458) or the plasmid expressing sgRNAs against CDK6 pSpCas9(BB)-2A-GFP(px458)-hCDK6del. For each transfection, $2x10^5$ cells were resuspended in Buffer R (Neon™) in a reaction volume of 10µl. Transfected cells were cultured in RPMI (supplemented with 10% FCS and 50 µmol/L 2-mercaptoethanol) for 24h. GFP^+ cells were sorted using a FACSAria™ II cell sorter (BD Biosciences, San Jose, CA, USA) and plated as single cell suspension into 96-well plates. For the re-expression of HA-CDK6, pMSCV-IRES-GFP plasmids were used. The outgrowth of clones was monitored by microscopic inspection. Cells are routinely tested for mycoplasma contamination.

RNA extraction and Real-Time PCR

Total RNA was extracted from cell lines using the RNeasy Mini Kit (Qiagen) as recommended by the manufacturer. Reverse transcription was performed using the iSCRIPT cDNA synthesis kit (Bio-Rad). All qPCRs were performed in duplicate with the SsoFastTM EvaGreen®Supermix (Bio-Rad) according to the instructions of the manufacturer. Primer sequences for Dnmt3b were as follows: fwd, 5´-GTGGTGCACTGAGCTCGAAAGGATCTTCG-3´ and rev, 5´-ATCACAGGCAAAGTAGTCCTTCAAGG-3´ (Kweon et al., 2017). Levels of mRNAs were normalized to Rplp0 mRNA.

Western Blotting

Protein lysates were prepared using RIPA lysis buffer supplemented with cOmplete™ Protease Inhibitor tablet (Roche Diagnostics, Indianapolis, IN, USA), separated by SDS/PAGE and transferred onto nitrocellulose blotting membrane (Amersham™ Protran™ 0.45µm NC, GE Healthcare, Life Sciences). Membranes were blocked in 5% BSA followed by incubation with primary antibodies: anti-CDK6 (1:1000, H-96, Santa Cruz, Dallas, TX, USA), anti-HA (1:1000, ab9110, Abcam, Cambridge, UK), anti-Dnmt3b (1:1000, ab122932, Abcam) and anti-HSC70 (1:1000, B-6, Santa Cruz). Appropriate secondary HRP antibodies (1:10000, Cell Signaling Technology, Danvers, MA, USA) were used and membranes were visualized using Clarity™ ECL Western blotting substrate (Biorad, Hercules, CA, USA).

Reduced Representation Bisulfite Sequencing (RRBS)

RRBS was performed as reported previously (Heller et al., 2016). In brief, genomic DNA was MspI (NEB) digested, end-repaired and A-tailed using Klenow Polymerase (NEB) followed by adapter ligation using Quick Ligase (NEB) and AMPure XP size selection (Beckman Coulter, Fullerton, CA, USA). RRBS libraries were sodium bisulfite treated using the EZ-DNA Methylation-Direct kit (Zymo Research Corp, Orange, CA, USA) and quantified by qPCR. Enrichment PCR was performed using the PfuTurboCx Hotstart Kit (Agilent Technologies, Santa Clara, CA, USA) followed by AMPure XP clean up. Quality of final RRBS libraries was determined by Experion analysis (Biorad). Sequencing was performed on a HiSeq2000 sequencer (Illumina Inc, San Diego, CA, USA). RRBS reads were processed using the --

rrbs option of the *Trim Galore!* software and *bismark* was used to align reads to GRCm38 and for methylation calling (Krueger and Andrews, 2011). Differential methylation analysis and data visualization were performed using the R packages *DSS* (v2.32.0), *methylKit* (v1.10.0), *EnhancedVolcano* (v1.2.0) and *ggplot2* (v3.2.1). RRBS data are deposited in the Gene Expression Omnibus (GEO) database (Accession ID: GSE145220).

RNA-seq

Total RNA was prepared using the RNeasy Kit (Qiagen) and processed for sequencing using the TruSeq RNA Sample Preparation Kit (Illumina Inc, San Diego, CA, USA). RNA-seq reads were processed using *Trim Galore!* software (http://www.bioinformatics.babraham.ac.uk/projects/trim_galore/) and aligned to GRCm38 using *STAR* (Dobin et al., 2013). Data visualization was done using ClustVis (Metsalu and Vilo, 2015). Gene Ontology analysis were performed using Ontologizer (Bauer et al., 2008) and visualized using the R package GOplot (Walter et al., 2015). RNA-seq data are deposited in the Gene Expression Omnibus (GEO) database (Accession ID: GSE156966, GSE145220).

ChIP-seq

CDK6 chromatin immunoprecipitation (ChIP) was performed using an antibody against HA (ab9110, Abcam) as described previously (Bellutti et al., 2018, Scheicher et al., 2015). Cells were crosslinked with DSG (20 minutes, RT) and 1% formaldehyde (10 minutes, RT) and termination of the fixation procedure was performed using glycine. For immunoprecipitation (IP), 70 µl Dynabeads Protein G magnetic beads (Invitrogen) were used, IP DNA was subjected to sequencing library preparation and sequencing was performed using the Illumina HiSeq3000/4000 platform. Raw sequencing reads were quality controlled using FASTQC followed by quality filtering, trimming of reads and adapter removal using trimmomatic (v0.36). Mapping against the mouse reference genome (Gencode M13) was done using bwa-mem (v0.7.15) and blacklisted regions were removed using bedtools subtract (v2.26.0). Multimappers and reads with bad mapping quality were removed using samtools (v1.3.1). Peak calling was performed by MACS2 (v2.1.0) using default parameters and motif identification was performed using Homer (v4.9.0) findMotifsGenome.pl with the default -size 200. ChIP-seq data are deposited in the Gene Expression Omnibus (GEO) database (Accession ID: GSE113752).

ATAC-seq

10^5 cells were washed once in 50 µl PBS and resuspended in transposase reaction mix (12.5 µl 2 × TD buffer, 2 µl transposase (Illumina), 10.5 µl nuclease-free water and 0.01% NP-40). Tagmentation was performed for 30 min at 37 °C. The optimum number of amplification cycles was estimated by qPCR reaction as previously described (Rendeiro et al., 2016). Following library amplification, fragments larger than 1 200 bp were excluded by SPRI size selection. DNA concentration was measured using a Qubit fluorometer (Invitrogen). Libraries were amplified using custom Nextera primers (Buenrostro et al., 2013) and sequenced by the Biomedical Sequencing Facility at CeMM using the Illumina HiSeq3000/4000 platform. ATAC-seq data are deposited in the Gene Expression Omnibus (GEO) database (Accession ID: GSE156966).

Chromatome analysis

Chromatome analyses were performed as described previously (Dutta et al., 2012, Bellutti et al., 2018). Briefly, the purified chromatin pellet was subjected to Benzonase digestion and solubilized in SDS lysis buffer. Filter Aided Sample Prep (FASP) was performed according to the procedure described previously (Wisniewski et al., 2009). Peptides were desalted using C18 solid phase extraction spin columns (The Nest Group, Southborough, MA) labeled with TMT 6plex™ reagents (Pierce, Rockford, IL) and pooled. Organic solvent was removed in vacuum concentrator and labelled peptides were loaded onto a solid phase extraction column. Peptides were eluted with 300µL 80% acetonitrile containing 0.1% trifluoroacetic to achieve a final peptide concentration of ~1µg/µl. Eluate was then used for phosphopeptide enrichment applying a modified method of immobilized metal affinity chromatography (IMAC) (Ficarro et al., 2005). Briefly, two times 100 µL of Ni-NTA superflow slurry (Qiagen) were washed with LCMS-grade water and Ni^{2+} stripped off the beads by incubation with 100 mM of EDTA, pH 8 solution for 1 h at room temperature. Stripped NTA resin was recharged with Fe^{3+}-ions by incubation with a fresh solution of $Fe(III)Cl_3$ and 75 µL of charged resin used for the enrichment of a total of ~300 µg TMT-labelled peptide. The unbound fraction was transferred to a fresh glass vial and used for offline fractionation for the analysis of the whole chromatome proteome. After washing the slurry with 0.1% TFA, phosphopeptides were eluted with a freshly prepared ammonia solution containing 3mM EDTA, pH 8 and all used for offline fractionation for the analysis of the phosphoproteome. Offline fractionation via RP-HPLC at pH 10 and 2D-RP/RP Liquid Chromatography Mass Spectrometry were performed as described (Bellutti et al., 2018). Raw data files were processed using the Proteome Discoverer 2.2.0. platform, utilizing the Sequest HT database search engine and Percolator validation software node

(V3.04) to remove false positives with a false discovery rate (FDR) of 1% on peptide and protein level under strict conditions. Searches were performed with full tryptic digestion against the mouse SwissProt database v2017.12 (25 293 sequences and appended known contaminants) with up to two miscleavage sites (Bellutti et al., 2018). For statistical analysis and p-value calculation, the integrated ANOVA hypothesis test was used. TMT ratios with p-values below 0.01 were considered statistically significant.

Publicly available datasets and co-expression analysis

The following human ALL Affymetrix HG-U133_plus_2.0 gene expression microarray datasets were obtained from ArrayExpress database: E-MTAB-5035, E-GEOD-13351, E-GEOD-49032 and E-GEOD-13576. Spearman correlation coefficients of log2 expression values were calculated using the “cor” function of R and data visualization was done using the “corrplot” package. ETS1 ChIP-seq data were obtained from GEO database: GSM803442, GSM803468, GSE83758. Infinium Human Methylation 450K BeadChip data of AML patients were obtained from the Cancer Genome Atlas database (LAML dataset).

SUPPLEMENTAL REFERENCES

BAUER, S., GROSSMANN, S., VINGRON, M. & ROBINSON, P. N. 2008. Ontologizer 2.0--a multifunctional tool for GO term enrichment analysis and data exploration. *Bioinformatics,* 24**,** 1650-1.

BELLUTTI, F., TIGAN, A. S., NEBENFUEHR, S., DOLEZAL, M., ZOJER, M., GRAUSENBURGER, R., HARTENBERGER, S., KOLLMANN, S., DOMA, E., PRCHAL-MURPHY, M., URAS, I. Z., HOLLEIN, A., NEUBERG, D. S., EBERT, B. L., RINGLER, A., MUELLER, A. C., LOIZOU, J. I., HINDS, P. W., VOGL, C., HELLER, G., KUBICEK, S., ZUBER, J., MALUMBRES, M., FARLIK, M., VILLUNGER, A., KOLLMANN, K. & SEXL, V. 2018. CDK6 Antagonizes p53-Induced Responses during Tumorigenesis. *Cancer Discov,* 8**,** 884-897.

BUENROSTRO, J. D., GIRESI, P. G., ZABA, L. C., CHANG, H. Y. & GREENLEAF, W. J. 2013. Transposition of native chromatin for fast and sensitive epigenomic profiling of open chromatin, DNA-binding proteins and nucleosome position. *Nat Methods,* 10**,** 1213-8.

DOBIN, A., DAVIS, C. A., SCHLESINGER, F., DRENKOW, J., ZALESKI, C., JHA, S., BATUT, P., CHAISSON, M. & GINGERAS, T. R. 2013. STAR: ultrafast universal RNA-seq aligner. *Bioinformatics,* 29**,** 15-21.

DUTTA, B., ADAV, S. S., KOH, C. G., LIM, S. K., MESHORER, E. & SZE, S. K. 2012. Elucidating the temporal dynamics of chromatin-associated protein release upon DNA digestion by quantitative proteomic approach. *J Proteomics,* 75**,** 5493-506.

FICARRO, S. B., SALOMON, A. R., BRILL, L. M., MASON, D. E., STETTLER-GILL, M., BROCK, A. & PETERS, E. C. 2005. Automated immobilized metal affinity chromatography/nano-liquid chromatography/electrospray ionization mass spectrometry platform for profiling protein phosphorylation sites. *Rapid Commun Mass Spectrom,* 19**,** 57-71.

HELLER, G., TOPAKIAN, T., ALTENBERGER, C., CERNY-REITERER, S., HERNDLHOFER, S., ZIEGLER, B., DATLINGER, P., BYRGAZOV, K., BOCK, C., MANNHALTER, C., HORMANN, G., SPERR, W. R., LION, T., ZIELINSKI, C. C., VALENT, P. & ZOCHBAUER-MULLER, S. 2016. Next-generation sequencing identifies major DNA methylation changes during progression of Ph+ chronic myeloid leukemia. *Leukemia,* 30**,** 1861-8.

KRUEGER, F. & ANDREWS, S. R. 2011. Bismark: a flexible aligner and methylation caller for Bisulfite-Seq applications. *Bioinformatics,* 27**,** 1571-2.

KWEON, S. M., ZHU, B., CHEN, Y., ARAVIND, L., XU, S. Y. & FELDMAN, D. E. 2017. Erasure of Tet-Oxidized 5-Methylcytosine by a SRAP Nuclease. *Cell Rep,* 21**,** 482-494.

METSALU, T. & VILO, J. 2015. ClustVis: a web tool for visualizing clustering of multivariate data using Principal Component Analysis and heatmap. *Nucleic Acids Res,* 43**,** W566-70.

RAN, F. A., HSU, P. D., WRIGHT, J., AGARWALA, V., SCOTT, D. A. & ZHANG, F. 2013. Genome engineering using the CRISPR-Cas9 system. *Nat Protoc,* 8**,** 2281-2308.

RENDEIRO, A. F., SCHMIDL, C., STREFFORD, J. C., WALEWSKA, R., DAVIS, Z., FARLIK, M., OSCIER, D. & BOCK, C. 2016. Chromatin accessibility maps of chronic lymphocytic leukaemia identify subtype-specific epigenome signatures and transcription regulatory networks. *Nat Commun,* 7**,** 11938.

SCHEICHER, R., HOELBL-KOVACIC, A., BELLUTTI, F., TIGAN, A. S., PRCHAL-MURPHY, M., HELLER, G., SCHNECKENLEITHNER, C., SALAZAR-ROA, M., ZOCHBAUER-MULLER, S., ZUBER, J., MALUMBRES, M., KOLLMANN, K. & SEXL, V. 2015. CDK6 as a key regulator of hematopoietic and leukemic stem cell activation. *Blood,* 125**,** 90-101.

WALTER, W., SANCHEZ-CABO, F. & RICOTE, M. 2015. GOplot: an R package for visually combining expression data with functional analysis. *Bioinformatics,* 31**,** 2912-4.

WISNIEWSKI, J. R., ZOUGMAN, A., NAGARAJ, N. & MANN, M. 2009. Universal sample preparation method for proteome analysis. *Nat Methods,* 6**,** 359-62.